https://doi.org/10.1016/j.foodhyd.2014.12.032

Submitted to *Food Hydrocolloids*

(Research manuscript)

Revised FOODHYD-D-14-00614R1

Characterization and antibacterial activity of silver nanoparticles prepared with a fungal exopolysaccharide in water

Xia Chen, Jing-Kun Yan, Jian-Yong Wu*

Department of Applied Biology & Chemical Technology, State Key Laboratory of Chinese Medicine and Molecular Pharmacology in Shenzhen, The Hong Kong Polytechnic University, Hung Hom, Kowloon, Hong Kong

*Corresponding author:

Tel.: (852)3400 8671; fax: (852) 2364 9932; e-mail: jian-yong.wu@polyu.edu.hk

Abstract

This work demonstrates a simple and feasible approach for the synthesis of silver nanoparticles (AgNPs) in water with a high molecular weight (MW) exopolysaccharide fraction, EPS1 produced by a medicinal fungus Cs-HK1. The formation and properties of AgNPs were evaluated at various temperatures, time periods, and silver nitrate/EPS1 concentrations in water. At suitable conditions (100 ^{o}C, 60 min and 10 mM $AgNO_3$ with 1.0 mg/mL EPS1), AgNPs were formed with an average diameter of 50 nm and a narrow size distribution, remaining as a stable dispersion for at least 2 months. EPS1 may be acting as a reducing and stabilizing agent for the formation of AgNPs, which were attached to the hydroxyl groups of EPS1. The AgNPs formed in EPS1 solution exhibited a concentration-dependent inhibition of both Gram-negative and -positive bacteria but a very low cytotoxicity on the RAW264.7 murine macrophage cells. The results demonstrated the feasibility for green synthesis of AgNPs as potential antibacterial agents using natural polysaccharides dissolved in water.

Keywords: silver nanoparticles, exopolysaccharide, medicinal fungus, antibacterial activity

1. Introduction

Silver nanoparticle (AgNP) has attracted enormous interest because of its great potential for wide applications in food, cosmetic, clothing and pharmaceutical industries (Ahamed, Alsalhi, & Siddiqui, 2010; Marambio-Jones & Hoek, 2010; Rai, et al., 2014). Many physical (Breitwieser, et al., 2013; Pal, Shah, & Devi, 2009) and chemical methods (Guzman, Dille, & Godet, 2012; Raveendran, Fu, & Wallen, 2003) have been exploited to produce AgNPs. Chemical reduction of Ag^+ ions is one of the most common approaches for AgNP synthesis, in which sodium borohydride, sodium citrate and dimethylformamide have been the highly reactive reducing agents (Leung, Wong, & Xie, 2010). However, some of the AgNPs formed with the small molecules as the reducing agents have been found to cause potent cytotoxicity (AshaRani, Low Kah Mun, Hande, & Valiyaveettil, 2009). A possible cause for the strong cytotoxicity of AgNPs is their rapid diffusion into cells (Travan, et al., 2009). Alternatively, biopolymers especially natural polysaccharides such as cellulose and chitosan have been applied to produce non-toxic and biocompatible AgNPs (Li, Zhang, Xu, & Zhang, 2011). Modified chitosan has been used to form well-dispersed non-toxic AgNPs in water (Travan, et al., 2009).

Microbial exopolysaccharides (EPS) are usually industrially produced by submerged fermentation, which have found wide applications in food and pharmaceutical inductury (Lehtovaara & Gu, 2011; Schmid, Meyer, & Sieber, 2011). AgNPs have been synthesized with an EPS extracted from a lactic acid bacterium, showing notable antimicrobial activity (Kanmani & Lim, 2013). Schizophyllan, a linear (1→3)-β-D-glucan with strong anticancer

and immunemodulatory activities produced by the medicinal fungus *Schizophyllum commune*, has been used to form non-toxic AgNPs with a diameter of 6 nm (Abdel-Mohsen, et al., 2014).

Cs-HK1 fungus is a species of *Cordyceps sinesis* (Berk.) Sacc., a valuable medicinal fungus generally known as the Chinese caterpillar fungus, and Cs-HK1 mycelial culture has been applied to liquid fermentation for production of fungal biomass and EPS (Leung, Zhang, & Wu, 2006; Yan, Wang, & Wu, 2014). EPS1 was a partially purified EPS fraction (~2,700 kD) isolated from Cs-HK1 mycelial fermentation broth, which was composed mainly of (1→3)-β-D-glucan with glucose side chains (Chen, Ding, Wang, Siu, & Wu, 2014) and about 27% (w/w) galactomannan-protein complexes (~50 kDa) (Chen, Siu, Cheung, & Wu, 2014). This study was carried out to evaluate the preparation and properties of AgNPs with EPS1 in an aqueous solution. The AgNPs prepared at various conditions were characterized using several instrumental methods and further evaluated for cytotoxicity and antibacterial activities.

2. Materials and methods

2.1 Fungal fermentation and EPS1 isolation

The Cs-HK1 fungus was previously isolated from the fruiting body of a natural *Cordyceps sinensis* (Leung, et al., 2006). Cs-HK1 mycelial liquid fermentation for EPS production was carried out in shake flasks at 20 ^{o}C for a period of 7 days. The fermentation liquid was then centrifuged, and the supernatant medium was collected for EPS isolation by ethanol

precipitation. The EPS1 used in this study was isolated from the medium by precipitation with 2/3 volume ratio of ethanol (95% grade) (~40% v/v), followed by dialysis and freeze drying as reported previously (Chen, Siu, et al., 2014). About 3.0 g/L of EPS1 was recovered from the Cs-HK1 fermentation broth, which was relatively high as compared with the EPS yields from mycelial fermentation of other medicinal fungi in the literature (Cui & Zhang, 2011; Lin, 2011; Zhang & Cheung, 2011).

2.2 Synthesis of AgNPs

The synthesis of AgNPs with EPS1 followed a reported procedure with minor modifications (Leung, et al., 2010). All the $AgNO_3$ and EPS1 solutions were prepared in distilled water. The $AgNO_3$ was purchased from Sigma-Aldrich (ACS reagent, #209139). The $AgNO_3$ solution (2 mL) at various concentrations was mixed with an equal volume of EPS1 solution at a selected concentration. The reaction mixture was incubated with constant stirring for 10 to 60 min at 25, 40, 60 or 100 ^{o}C in the dark. After completion of the reaction, the solution was stored at room temperature (~25 ^{o}C) in the dark before use.

2.3 Characterization of AgNPs

The UV-Vis spectra of AgNPs and EPS1 in water were measured from 300-600 nm on a HEWLETT Packard 8453 spectrophotometer against pure EPS1 solution as the blank. Dynamic light scattering (DLS) measurement was performed of AgNPs at 25 ^{o}C on a Malvern Zetasizer Nano (Malvern Instruments Ltd., UK) at 632.8 nm and 90^{o} scattering angle. The particle size, morphology and selected-area electron diffraction (SAED) of AgNPs

were observed by field emission electron microscope (JEOL model JEM-2100F). TEM samples were prepared by placing a drop of sample solution on the carbon coated copper grids and vacuum dried. Silver content was determined by ICP-OES (Agilent Technologies 700 Series). Standard solutions were prepared by 0-2.0 mM silver nitrate solution. Infrared (IR) spectra were measured at room temperature from 4000-500 cm^{-1} at 4 cm^{-1} resolution with baseline corrected on a Perkin-Elmer 1600 instrument.

2.4 Cytotoxicity assay

The murine macrophage cell line RAW264.7 was employed for the cytotoxicity assay. The RAW264.7 cells were maintained in DMEM medium containing 10% FBS (v/v), 2 mM L-glutamine and antibiotics (100 U/mL penicillin, 100 μg/mL streptomycin) (Gibco BRL, U.S.A.). Cells were cultured in a humidified incubator at 37 ^{o}C with 5% CO_2. For the assay, 0.5×10^4 of RAW264.7 cells were grown in DMEM medium containing the AgNPs/EPS1 samples at chosen concentrations. Cell viability was determined by the colorimetric 3-(4,5-dimethylthiazol-2-yl)-2,5-diphenyl- tetrazolium bromide (MTT) method (Mosmann, 1983). The morphology of cells was observed by a microscope (Olympus IX51, Japan).

2.5 Antibacterial assay

Escherichia coli (Gram-negative) and *Staphylococcus aureus* (Gram-positive) were used in the antibacterial tests. The *in vitro* antibacterial activity was conducted in 96-well microplates using the broth micro-dilution procedure according to the Clinical and Laboratory Standards Institute guidelines (Jorgensen & Hindler, 2007). Four to five colonies from overnight

cultures of the test bacteria on a tryptone (Fluka, Analytical, Sigma-Aldrich Co., USA) agar plate were inoculated in 10 mL of Luria-Bertani broth at 37 ^{o}C for 4-6 h. The bacterial suspension was inoculated into a 96-well microplate (final concentration of ~10^5 CFU/mL) containing 100 μL of serial dilutions of the tested samples. After incubation for 12 h at 37 ^{o}C, the absorbance at 600 nm (A_{600}) was recorded to calculate the percentage of bacteria cell inhibition with respect to the untreated control, using a microplate reader (Chan, et al., 2013). The assay of each sample was performed in triplicate.

3. Results and discussion

3.1 Optical properties of AgNPs

Fig. 1 shows the UV-Vis spectra of $AgNO_3$ and EPS1 mixture solutions in water prepared at various concentrations, temperatures and time periods. When Ag ion is reduced to Ag atom in a solution, the colorless solution is turned into yellowish brown. An absorption band is an indication of AgNP formation in the solution (Xu, et al., 2014), which can be detected by the surface plasmon resonance (SPR) band using UV-Vis spectroscopy (Kanmani, et al., 2013). In this study, the AgNPs formed in EPS1 solution showed a strong SPR peak at about 410 nm (Fig. 1). The formation of AgNPs was due probably to the reduction of Ag^+ ions into Ag atoms by the EPS1 added to the $AgNO_3$ solution.

The absorption intensity of $AgNO_3$-EPS1 mixture solution initially increased and then decreased with the increase of EPS1 concentration from 0.01 mg/mL to 2.0 mg/mL (Fig. 1A), indicating the increase or decrease in the concentration of AgNPs formed. The similar trend

of UV-Vis absorption change has also been reported previously (Wu, Zhang, & Zhang, 2012), due probably to the formation of large particles or clusters by the prepared AgNPs. Fig. 1B shows the UV-Vis absorption of AgNPs prepared with 1.0 mg/mL EPS1 and various concentrations of $AgNO_3$. Relatively high absorption intensities attained at 4 mM and 6 mM $AgNO_3$ but with notable background noise, which was due probably to the poor stability of AgNPs formed (Wei, Sun, Qian, Ye, & Ma, 2009). The most symmetrical absorption peak was observed with 10 mM $AgNO_3$, indicating more uniform AgNPs (Wu, et al., 2012). SPR absorption of AgNPs is sensitive to variations in physical properties and aggregation of particles in solution (Liu, Lee, Kim, & Kim, 2007). Chemical modification of the particle surface may be effective to attain uniform particle size and avoid aggregation. Fig. 1C shows the UV-Vis absorption spectra of AgNPs prepared at various temperatures (and a fixed reaction time of 20 min), showing no absorption band until the temperature was increased to 100 ^{o}C. In our preliminary experiments (data not shown), absorption band was also observed at 80 ^{o}C with a longer reaction time of 40 min. The results suggested that the effect of temperature on the formation of AgNPs in the EPS1 solution was mainly attributed to its influence on the reaction rate of Ag ions reduction. Similarly, formation of AgNPs using sophorolipids as reducing and capping agent was not observed until the temperature was increased to 90 ^{o}C (Kasture, et al., 2008). Fig. 1D shows the UV-Vis spectra of AgNPs prepared in EPS1 solution for different periods of time, exhibiting a stronger absorbance (more AgNPs formed) with longer time of heat treatment. The experimental results altogether suggested that the most favorable reaction conditions for formation of uniform AgNPs were

10 mM $AgNO_3$, 1.0 mg/mL EPS1 at 100 ^oC for 60 min. AgNPs formed at this set of conditions were used in the following morphology analysis and bioactivity tests.

3.2 FT-IR spectra of AgNPs

FT-IR measurements were carried out to detect the possible reactions for the reduction of Ag ions and stabilization of Ag atoms in EPS1 (Fig. 2A). The peaks at 3000-3600 cm^{-1} corresponded to the stretching vibrations of hydroxyl groups and amine groups. Usually the wave numbers of N-H is lower than that of O-H (Pawlak & Mucha, 2003). The peak at 3407 cm^{-1} in the spectrum of EPS1 can be attributed to the N-H in the proteins and the shift of N-H still was 3407 cm^{-1} in the spectrum of AgNPs. The absorption peak at 3482 cm^{-1} in the spectrum of EPS1 was attributed to the stretching vibration of O-H. The peak shifted to lower wavenumbers (3458 cm^{-1}) in the spectrum of AgNPs, suggesting the interactions between hydroxyl groups of EPS1 and the AgNPs (Yan, et al., 2013). This observation can be further verified by the shift of the deformation vibration of O-H at about 1100 cm^{-1}. The slightly red shift from 1078 cm^{-1} to 1074 cm^{-1} was also indicating the interaction of hydroxyl groups of EPS1 and the AgNPs (Li, et al., 2011). No obvious difference shown at about 1380 cm^{-1} revealed the excess of $AgNO_3$ had been removed by dialysis (Sedenkova, Trchova, Stejskal, & Prokes, 2009). The peak at 889 cm^{-1} was indicative of β-configuration in the polysaccharide structures of EPS1 (Cael, Koenig, & Blackwel.J, 1974).

3.3 Element composition and morphology properties of AgNPs

The content of atomic silver in the prepared nanoparticles was detected by ICP-OES. Excess silver ions were removed by dialysis with MWCO 3000 dialysis bag. After this, content of silver was about 6.7% (w/w) in the prepared AgNPs. After filtration through 0.22 μm membrane, 2.3% (w/w) of silver was found in the AgNPs sample and the color of AgNPs solution was much light. About 2/3 of silver atoms was removed by micro-filtration.

As shown in Fig. 2B, the particle size of EPS1 was about 1650 nm. After the reaction, the particle size of the AgNPs was 450 nm, which was much larger than the filtrated AgNPs solution (120 nm). Degradation and conformation change of the polysaccharide chains are two most possible causes for the size reduction of polysaccharide aggregates in water. However, in our preliminary test, the MW of EPS1 did not change after placed in hot water (100 ^{o}C) for several hours. Therefore, the size reduction during the formation of AgNPs was most probably attributed to conformation changes in the polysaccharide chains. The chain of the excess polysaccharides in EPS1 was closer after the reduction due to the attached silver atoms. Although the particle size of AgNPs determined by DLS was inaccurate owing to the large particle size of EPS1, only a symmetrical peak of AgNPs was observed in Fig. 2B, indicating the synthesized AgNPs were attached to the chains of the excess polysaccharides.

TEM provided further insight into the morphology and size details of the formed AgNPs (Fig. 3). Histograms of particle size distribution were obtained by counting more than 100 silver nanoparticles in several TEM images (Fig. 4). Most particles were around 40 nm in the newly prepared AgNPs (Fig. 3A & Fig. 4A) although some larger particles (>70 nm) were also

observed. After filtration with 0.22 μm membrane, some large particles were removed and most particles were around 30-40 nm (Fig. 3B & Fig. 4B). The larger particle size of AgNPs detected by DLS was probably attributed to the aggregation of excess polysaccharides in the solution according to the TEM result reported previously (Li, Wang, Cui, Huang, & Kakuda, 2006). Denaturation has been observed during the formation of AgNPs in xanthan solution and after stored for 1 week, the renaturation of xanthan due to intra- and inter-molecular hydrogen bonds induced the aggregation of the formed nanoparticles (Xu, et al., 2014). In contrast, AgNPs formed in EPS1 solution in this study remained well dispersed in the solution after 2 months without any significant change in the particle size distribution (Fig. 3A & Fig. 3C; Fig. 4A & Fig. 4C). As suggested by Li et al. (Li, et al., 2011), the stable AgNPs formed in lentinan [a (1→3)-β-D-glucan] solution were attributed to the provision of a matrix for the formation of AgNPs and a stabilizer for good dispersion by the polysaccharides. Similarly, the main component of EPS1 was a (1→3)-β-D-glucan (Chen, Siu, et al., 2014), which may present a triple-helix conformation for formation and stabilization of AgNPs in an aqueous solution (Li, et al., 2011). The SAED pattern of AgNPs showed concentric rings resulting from the random orientation of crystal planes (Fig. 3A, inset), suggesting that AgNPs existed as polycrystalline metallic rather than non-crystalline NPs.

Based on the above results from FT-IR, DLS and TEM, we proposed a schematic model to describe the binding of AgNPs to EPS1 in Fig. 5. As EPS1 was composed of (1→3)-β-D-glucans (Chen, Siu, et al., 2014) and galactomannan-protein complexs (Chen, Ding, Wang, Siu, & Wu, 2014), (1→3)-β-D-glucans usually form triple helixes and the

231 galactomannan-protein complexes can form random coils in an aqueous solution (Andrade,
232 Azero, Luciano, & Goncalves, 1999). A purified, ultrasound-degraded fraction of EPS1
233 (called EPS1U, ~730 kD) consisting of (1→3)-β-D-glucan was also tested for the synthesis of
234 AgNPs, though the reduction rate of silver ions was much lower than that using EPS1
235 (Supplementary Fig. 1). This suggests that the other constituents of EPS1, namely the
236 polysaccharide-protein complexes, improved the reduction of silver ions to form AgNPs.
237 These lower MW polysaccharide-protein complexes may be attached to the triple-helix
238 formed by the β-glucan chains and ion charges on the proteins can attract the silver ions. As
239 reported previously (Travan, et al., 2009), AgNPs can interact with nitrogen atoms in the
240 modified chitosan (Chitlac) and the exterior amino groups in Chitlac can contribute to
241 prevent the aggregation of metal nanoparticles. In this study, only interactions between O-H
242 and AgNPs were observed.
243
244 *3.4 Cytotoxicity of AgNPs*
245 On the basis of aforementioned results, both the content of silver and the particle size of
246 AgNPs changed after filtration. Therefore, samples used in the cytotoxicity study and
247 antibacterial test were autoclave sterilized instead of membrane filtration. The cytotoxicity of
248 EPS1 was also detected to eliminate the effect of excess EPS1 in AgNPs. As shown in Table
249 1, treatment with AgNPs for 24 h showed no significant cytotoxicity to RAW264.7 cells.
250 However, when the treatment period was extended to 48 h, the growth of RAW264.7 cells
251 was inhibited significantly. EPS1 (5 mg/mL) alone did not cause any significant cytotoxicity
252 to RAW264.7 cells. The effect of AgNPs and EPS1 treatment on the morphology was also

observed (Supplementary Fig. 2). The morphology of cells was not significantly influenced by treatment with AgNPs at the lower concentration (0.5 mg/mL) or shorter period (24 h) in comparison with the healthy control cells. The cells were notably deformed with AgNPs at the higher concentration (5 mg/mL) and longer treatment period (48 h). Treatment with EPS1 did not affect the growth of RAW264.7 cells even at the high concentration (5 mg/mL). The microscopic observation was in general agreement with the above results of cytotoxicity test by MTT assay.

3.5 Antibacterial activities of AgNPs

AgNPs completely inhibited the growth of *E. coli* at 1.6 mg/mL and *S. aureus* at 0.8 mg/mL (Table 1). The results showed that AgNPs can inhibit Gram-positive bacteria more than Gram-negative bacteria. EPS1 alone did not inhibit any of bacteria (Table 1).

Although various EPS have been used to produce AgNPs with antimicrobial activities (Rai, et al., 2014), the strong cytotoxicity of AgNPs affected their application (AshaRani, et al., 2009). Although non-cytotoxic AgNPs have been reported, the content of silver atoms in the prepared silver nanoparticles was unknown (Abdel-Mohsen, et al., 2014; Travan, et al., 2009). In this study, we used ICP-OES to determine the concentration of silver in the prepared AgNPs. AgNPs at 0.8 mg/mL have been shown to have notable antibacterial activity but low cytotoxicity during 24 h treatment. Further study is needed to gain better understanding of the properties of AgNPs, to improve the antibacterial activity and to reduce the toxicity.

4. Conclusions

In this study, AgNPs were synthesized using an EPS fraction produced by a medicinal fungus Cs-HK1 in liquid fermentation. Fairly uniform, stable and well-dispersed AgNPs could be formed with suitable conditions including $AgNO_3$ and EPS1 concentrations, reaction time and temperature. The synthesis procedure was simple and also green using water as the sole reaction solvent without any other chemical agents or organic solvents. Moreover, AgNPs formed with EPS1 exhibited significant antibacterial activity against both Gram-positive and Gram-negative pathogenic bacteria with very low cytotoxicity, suggesting the great potential for application in the food and pharmaceutical industry. There is still a need to investigate the reaction mechanisms and physical interactions between Ag ions/Ag atoms and EPS1 constituents responsible for the formation of AgNPs in EPS1 solution and to optimize the yield and quality of AgNPs.

Acknowledgments

This work was supported by grants from the Hong Kong Government UGC (GRF Projects PolyU 5036/10P and PolyU 5033/11P) and from The Hong Kong Polytechnic University.

References

Abdel-Mohsen, A. M., Abdel-Rahman, R. M., Fouda, M. M. G., Vojtova, L., Uhrova, L., Hassan, A. F., Al-Deyab, S. S., El-Shamy, I. E., & Jancar, J. (2014). Preparation, characterization and cytotoxicity of schizophyllan/silver nanoparticle composite. *Carbohydrate Polymers, 102*, 238-245.

Ahamed, M., Alsalhi, M. S., & Siddiqui, M. K. (2010). Silver nanoparticle applications and human health. *Clin Chim Acta, 411*(23-24), 1841-1848.

Andrade, C. T., Azero, E. G., Luciano, L., & Goncalves, M. P. (1999). Solution properties of the galactomannans extracted from the seeds of Caesalpinia pulcherrima and Cassia javanica: comparison with locust bean gum. *International Journal of Biological Macromolecules, 26*(2-3), 181-185.

AshaRani, P. V., Low Kah Mun, G., Hande, M. P., & Valiyaveettil, S. (2009). Cytotoxicity and genotoxicity of silver nanoparticles in human cells. *ACS Nano, 3*(2), 279-290.

Breitwieser, D., Moghaddam, M. M., Spirk, S., Baghbanzadeh, M., Pivec, T., Fasl, H., Ribitsch, V., & Kappe, C. O. (2013). In situ preparation of silver nanocomposites on cellulosic fibers--microwave vs. conventional heating. *Carbohydr Polym, 94*(1), 677-686.

Cael, J. J., Koenig, J. L., & Blackwel.J. (1974). Infrared and Raman-Spectroscopy of Carbohydrates .4. Identification of Configuration-Sensitive and Conformation-Sensitive Modes for D-Glucose by Normal Coordinate Analysis. *Carbohydrate Research, 32*(1), 79-91.

Chan, F. Y., Sun, N., Neves, M. A. C., Lam, P. C. H., Chung, W. H., Wong, L. K., Chow, H. Y., Ma, D. L., Chan, P. H., Leung, Y. C., Chan, T. H., Abagyan, R., & Wong, K. Y. (2013). Identification of a New Class of FtsZ Inhibitors by Structure-Based Design and in Vitro Screening. *Journal of Chemical Information and Modeling, 53*(8), 2131-2140.

Chen, X., Ding, Z. Y., Wang, W. Q., Siu, K. C., & Wu, J. Y. (2014). An antioxidative galactomannan-protein complex isolated from fermentation broth of a medicinal fungus Cs-HK1. *Carbohydrate Polymers, 112*, 469-474.

Chen, X., Siu, K. C., Cheung, Y. C., & Wu, J. Y. (2014). Structure and properties of a (1-->3)-beta-D-glucan from ultrasound-degraded exopolysaccharides of a medicinal fungus. *Carbohydr Polym, 106*, 270-275.

Cui, J. D., & Zhang, B. Z. (2011). Comparison of culture methods on exopolysaccharide production in the submerged culture of Cordyceps militaris and process optimization. *Lett Appl Microbiol, 52*(2), 123-128.

Guzman, M., Dille, J., & Godet, S. (2012). Synthesis and antibacterial activity of silver nanoparticles against gram-positive and gram-negative bacteria. *Nanomedicine-Nanotechnology Biology and Medicine, 8*(1), 37-45.

Jorgensen, J. H., & Hindler, J. F. (2007). New consensus guidelines from the Clinical and Laboratory Standards Institute for antimicrobial susceptibility testing of infrequently isolated or fastidious bacteria. *Clinical Infectious Diseases, 44*(2), 280-286.

Kanmani, P., & Lim, S. T. (2013). Synthesis and structural characterization of silver nanoparticles using bacterial exopolysaccharide and its antimicrobial activity against food and multidrug. resistant pathogens. *Process Biochemistry, 48*(7), 1099-1106.

Kasture, M. B., Patel, P., Prabhune, A. A., Ramana, C. V., Kulkarni, A. A., & Prasad, B. L. V. (2008). Synthesis of silver nanoparticles by sophorolipids: Effect of temperature and sophorolipid structure on the size of particles. Journal of Chemical Scienes, 120(6), 512-520.

Lehtovaara, B. C., & Gu, F. X. (2011). Pharmacological, structural, and drug delivery properties and applications of 1,3-beta-glucans. *J Agric Food Chem, 59*(13), 6813-6828.

Leung, P. H., Zhang, Q. X., & Wu, J. Y. (2006). Mycelium cultivation, chemical composition and antitumour activity of a Tolypocladium sp. fungus isolated from wild Cordyceps sinensis. *J Appl Microbiol, 101*(2), 275-283.

Leung, T. C. Y., Wong, C. K., & Xie, Y. (2010). Green synthesis of silver nanoparticles using biopolymers, carboxymethylated-curdlan and fucoidan. *Materials Chemistry and Physics, 121*(3), 402-405.

Li, S., Zhang, Y. Y., Xu, X. J., & Zhang, L. N. (2011). Triple Helical Polysaccharide-Induced Good Dispersion of Silver Nanoparticles in Water. *Biomacromolecules, 12*(8), 2864-2871.

Li, W., Wang, Q., Cui, S. W., Huang, X., & Kakuda, Y. (2006). Elimination of aggregates of (1 -> 3) (1 -> 4)-beta-glucan in dilute solutions for light scattering and size exclusion chromatography study. *Food Hydrocolloids, 20*(2-3), 361-368.

Lin, E. S. (2011). Production of exopolysaccharides by submerged mycelial culture of Grifola frondosa TFRI1073 and their antioxidant and antiproliferative activities. *World Journal of Microbiology & Biotechnology, 27*(3), 555-561.

Liu, J., Lee, J. B., Kim, D. H., & Kim, Y. (2007). Preparation of high concentration of silver colloidal nanoparticles in layered laponite sol. *Colloids and Surfaces a-Physicochemical and Engineering Aspects, 302*(1-3), 276-279.

Marambio-Jones, C., & Hoek, E. M. V. (2010). A review of the antibacterial effects of silver nanomaterials and potential implications for human health and the environment. *Journal of Nanoparticle Research, 12*(5), 1531-1551.

Mosmann, T. (1983). Rapid colorimetric assay for cellular growth and survival: application to proliferation and cytotoxicity assays. *J Immunol Methods, 65*(1-2), 55-63.

Pal, A., Shah, S., & Devi, S. (2009). Microwave-assisted synthesis of silver nanoparticles using ethanol as a reducing agent. *Materials Chemistry and Physics, 114*(2-3), 530-532.

Pawlak, A., & Mucha, A. (2003). Thermogravimetric and FTIR studies of chitosan blends. *Thermochimica Acta, 396*(1-2), 153-166.

Rai, M., Kon, K., Ingle, A., Duran, N., Galdiero, S., & Galdiero, M. (2014). Broad-spectrum bioactivities of silver nanoparticles: the emerging trends and future prospects. *Appl Microbiol Biotechnol, 98*(5), 1951-1961.

Raveendran, P., Fu, J., & Wallen, S. L. (2003). Completely "green" synthesis and stabilization of metal nanoparticles. *Journal of the American Chemical Society, 125*(46), 13940-13941.

Schmid, J., Meyer, V., & Sieber, V. (2011). Scleroglucan: biosynthesis, production and application of a versatile hydrocolloid. *Applied Microbiology and Biotechnology, 91*(4), 937-947.

Sedenkova, I., Trchova, M., Stejskal, J., & Prokes, J. (2009). Solid-state reduction of silver nitrate with polyaniline base leading to conducting materials. *ACS Appl Mater Interfaces, 1*(9), 1906-1912.

Travan, A., Pelillo, C., Donati, I., Marsich, E., Benincasa, M., Scarpa, T., Semeraro, S., Turco, G., Gennaro, R., & Paoletti, S. (2009). Non-cytotoxic Silver Nanoparticle-Polysaccharide Nanocomposites with Antimicrobial Activity. *Biomacromolecules, 10*(6), 1429-1435.

Wei, D. W., Sun, W. Y., Qian, W. P., Ye, Y. Z., & Ma, X. Y. (2009). The synthesis of chitosan-based silver nanoparticles and their antibacterial activity. *Carbohydrate Research, 344*(17), 2375-2382.

Wu, J., Zhang, F., & Zhang, H. B. (2012). Facile synthesis of carboxymethyl curdlan-capped silver nanoparticles and their application in SERS. *Carbohydrate Polymers, 90*(1), 261-269.

Xu, W., Jin, W., Lin, L., Zhang, C., Li, Z., Li, Y., Song, R., & Li, B. (2014). Green synthesis of xanthan conformation-based silver nanoparticles: antibacterial and catalytic application. *Carbohydr Polym, 101*, 961-967.

Yan, J. K., Cai, P. F., Cao, X. Q., Ma, H. L., Zhang, Q., Hu, N. Z., & Zhao, Y. Z. (2013). Green synthesis of silver nanoparticles using 4-acetamido-TEMPO-oxidized curdlan. *Carbohydrate Polymers, 97*(2), 391-397.

Yan, J. K., Wang, W. Q., & Wu, J. Y. (2014). Recent advances in Cordyceps sinensis polysaccharides: Mycelial fermentation, isolation, structure, and bioactivities: A review. *Journal of Functional Foods, 6*, 33-47.

Zhang, B. B., & Cheung, P. C. K. (2011). A mechanistic study of the enhancing effect of Tween 80 on the mycelial growth and exopolysaccharide production by Pleurotus tuber-regium. *Bioresource Technology, 102*(17), 8323-8326.

Table Captions

Table 1 Inhibition and antimicrobial activity of EPS1 and AgNPs

Table 1

Sample	CC_{50} [a] (mg/mL)		MIC [b] (mg/mL)	
	24 h	48 h	*E. coli*	*S. aureus*
EPS1	> 5.0	> 5.0	> 5.0	> 5.0
AgNPs	> 5.0	0.5 ± 0.1	1.6 ± 0.3	0.8 ± 0.1

[a] The 50% cytotoxic concentration of samples on RAW264.7 cells.

[b] Minimum inhibitory concentration of samples.

<Figure Captions>

Figure 1. UV-Vis light absorbance spectra of $AgNO_3$ and EPS1 mixture reaction solution in various conditions: (A) 10 mM $AgNO_3$ with various concentrations of EPS1; (B) 1.0 mg/mL EPS1 with various concentrations of $AgNO_3$; (C) 10 mM $AgNO_3$ and 1.0 mg/mL EPS1 at various temperatures; (D) 10 mM $AgNO_3$ and 1.0 mg/mL EPS1 for various periods of reaction time.

Figure 2. Analysis of AgNPs formed in EPS1 solution: (A) FT-IR spectra of EPS1 and AgNPs; (B) particle size distribution of EPS1 and AgNPs (1.0 mg/mL) in water (by DLS performed at 25 ^{o}C and 90° scattering angle). (AgNPs prepared with 10 mM $AgNO_3$ and 1.0 mg/mL EPS1 at 100 ^{o}C for 60 min).

Figure 3. TEM images: (A) freshly prepared AgNPs; (B) freshly prepared AgNPs after filtration through 0.22 μM filter; (C) AgNPs stored for 2 months at 4 ^{o}C. (AgNPs prepared with 1.0 mg/mL EPS1 and 10 mM $AgNO_3$ at 100 ^{o}C and 60 min; inset: the electron diffraction pattern of particles).

Figure 4. Particles size distribution histogram determined from the TEM micrograph: (A) freshly prepared AgNPs; (B) AgNPs after filtration through 0.22 μM filter; (C) AgNPs stored for 2 months at 4 ^{o}C. (AgNPs prepared with 1.0 mg/mL EPS1 and 10 mM $AgNO_3$ at 100 ^{o}C and 60 min).

Figure 5. Schematic model to describe the binding of AgNPs to EPS1. Small coils attached to the triple helix are lower MW galactomannan-protein complexes and heteroglycans contained in EPS1.

Figure 1

Fig. 1

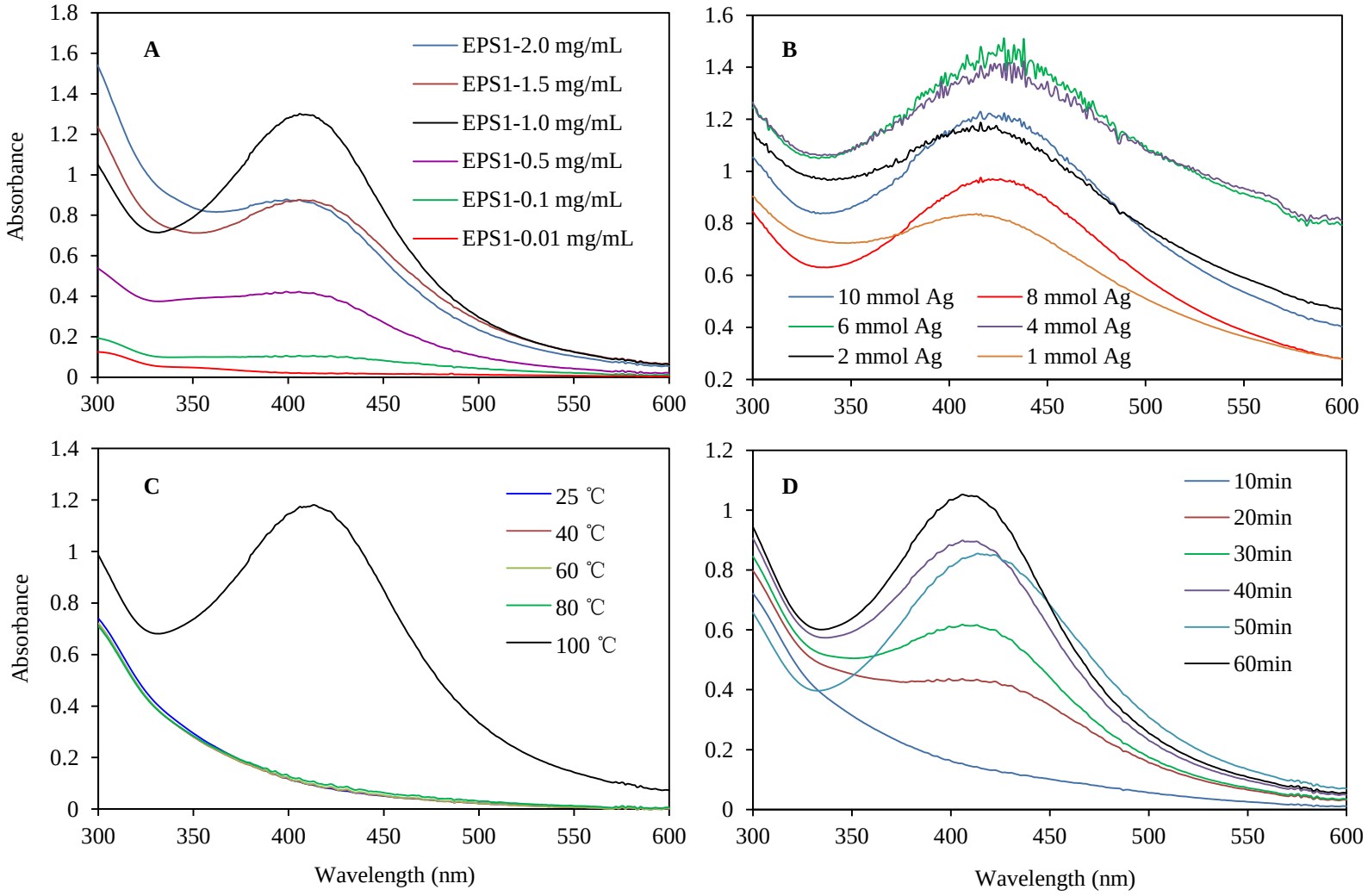

Figure 2

Fig. 2

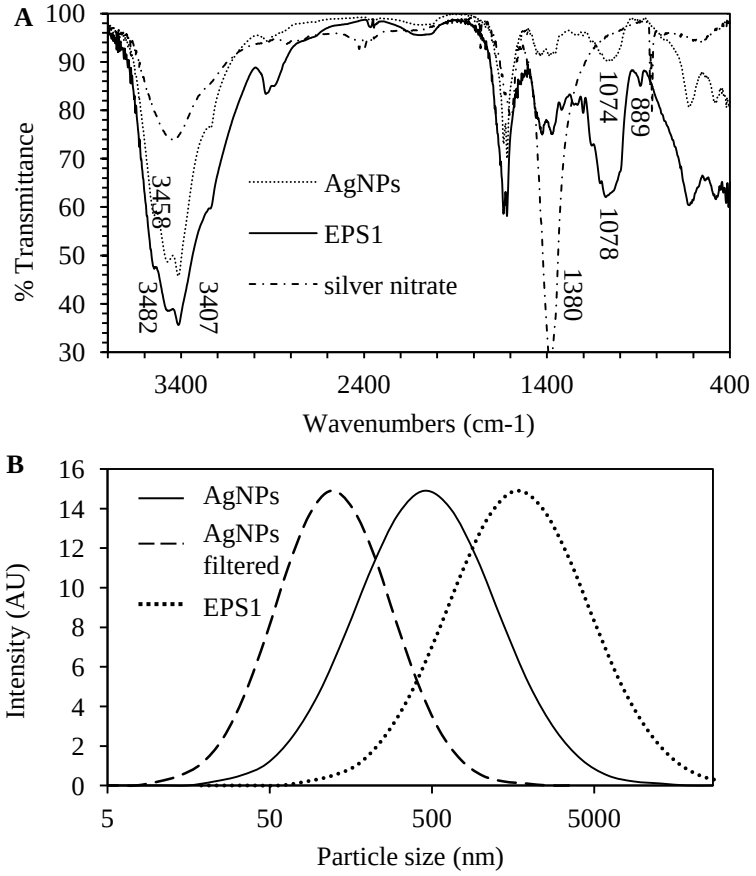

Figure 3

Fig. 3

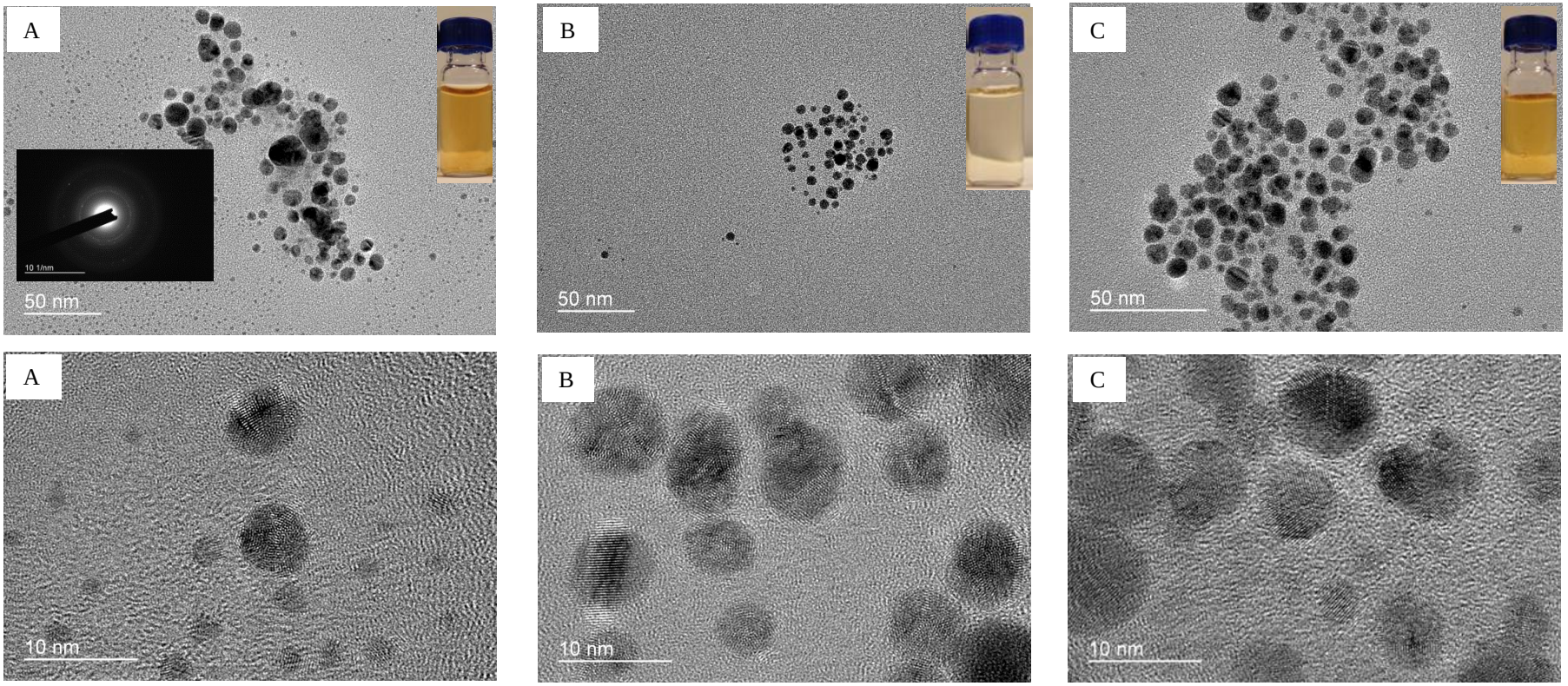

Figure 4

Fig. 4

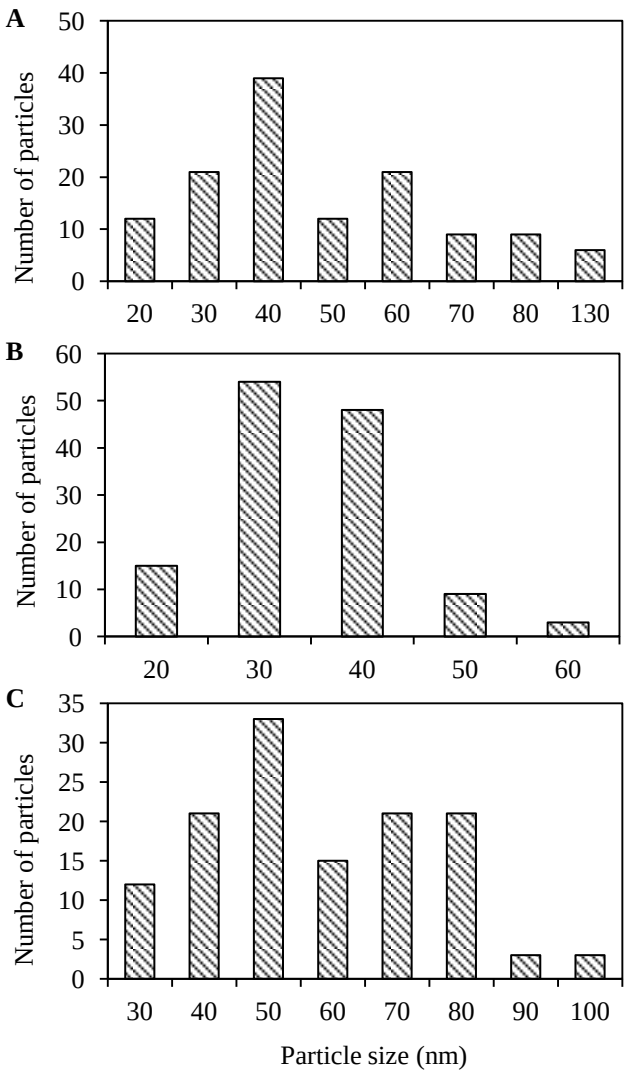

Figure 5

Fig. 5

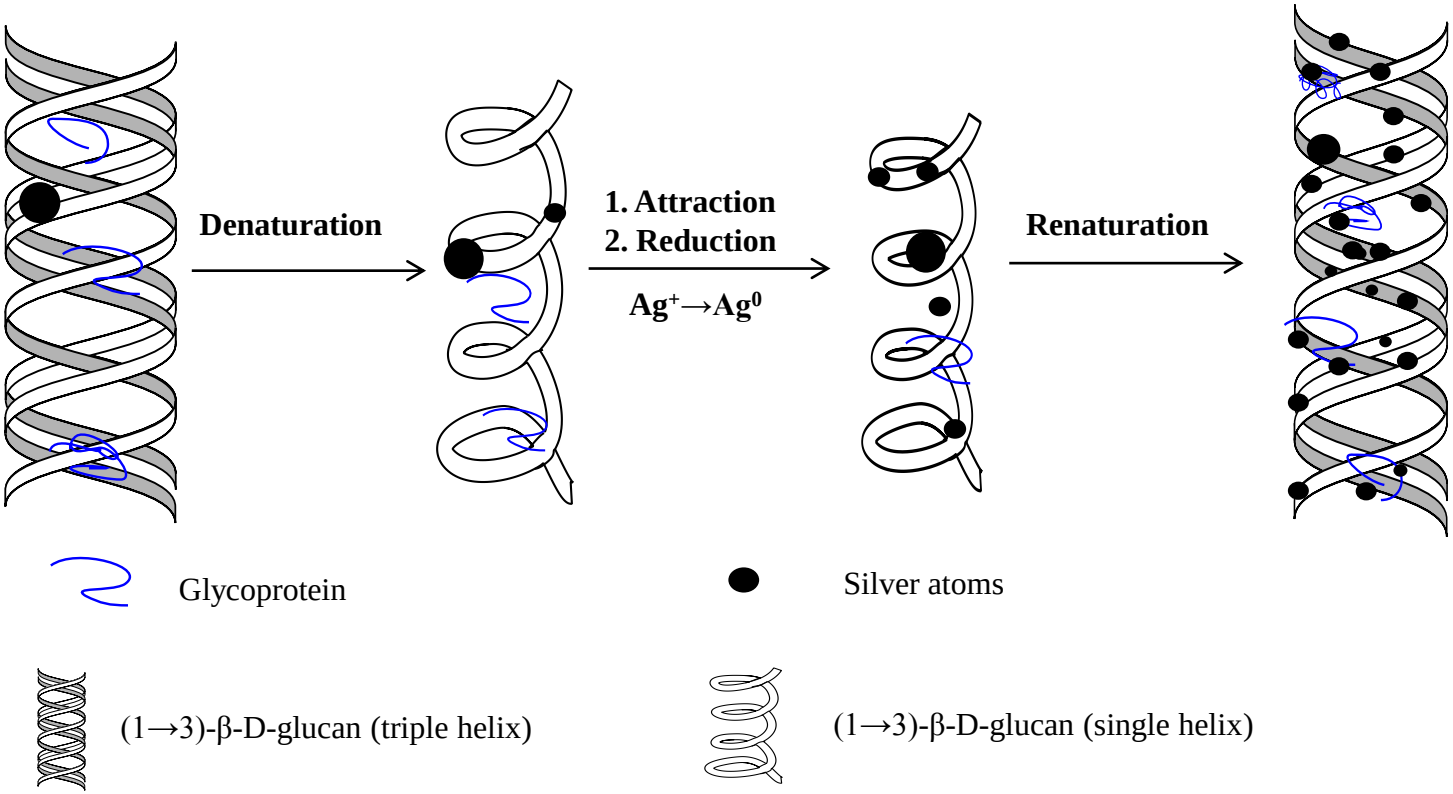

Fig. 1 UV-vis spectra of silver nanoparticles formed in EPS1U solution under the same conditions as EPS1 in different time. EPS1U was a purified fraction by gel filtration (S-300 HR) of the ultrasound-degraded EPS1 product as described in details by Chen, X, Siu, K. C., Cheung, Y. C., & Wu, J. Y. (2014) *Carbohydr Polym, 106*, 270-275.

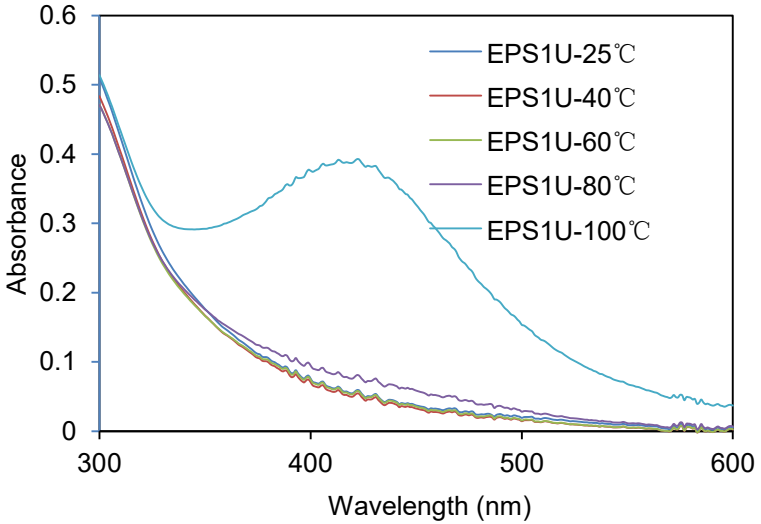

Fig. 2 Morphology of RAW264.7 cells